STUDY OF ACOUSTO-OPTICAL PROPERTIES OF CRYSTALS USING MACH–ZEHNDER INTERFEROMETER

Ulugbek Abdirakhmonov[1], Makset Nsanbayev[2]

[1]Navoi State University of Mining and Technologies. Navoiy. Uzbekistan

[2]Nukus state pedagogical institute. Nukus. Uzbekistan

**ulugbekabdiraxmonov@gmail.com*

Abstract. This paper presents a comprehensive investigation of the acousto-optic (AO) properties of lithium niobate ($LiNbO_3$), lithium tantalate ($LiTaO_3$), and langasite ($La_3Ga_5SiO_{14}$) crystals using the Mach–Zehnder interferometric technique. The method enables precise measurement of phase modulation and effective photoelastic coefficients (p_{eff}), allowing the evaluation of the acousto-optic figure of merit (M^2) and its anisotropy. Experimental measurements were performed in the frequency range of 400–1200 MHz using a helium–neon laser (λ = 633 nm). The results reveal a strong dependence of AO efficiency on crystal orientation, confirming theoretical predictions based on the Dixon–Cohen model. Lithium niobate exhibited the highest M^2 value, indicating its superior potential for acousto-optic modulators and deflectors. The findings validate the reliability of the Mach–Zehnder interferometric approach for characterizing anisotropic acousto-optic phenomena.

Keywords. Acousto-optics; Mach–Zehnder interferometer; Lithium niobate; Lithium tantalate; Langasite; Photoelastic coefficient; Figure of merit; Anisotropy.

Introduction

The study of acousto-optic (AO) characteristics of crystals has become increasingly significant due to their extensive use in optical communication, laser

modulation, and photonic signal control. Among the available experimental methods, the Mach–Zehnder interferometric approach holds particular importance as it enables highly precise analysis of phase modulation, effective photoelastic constants, and anisotropy in acousto-optic behavior.

The origins of acousto-optics trace back to the pioneering works of Debye and Sears [1], along with Lucas and Biquard [2], who first demonstrated the phenomenon of light diffraction by ultrasonic waves. Later, Dixon and Cohen [3] developed theoretical foundations that made it possible to calculate anisotropic photoelastic and AO parameters.

Crystals such as lithium niobate ($LiNbO_3$) and lithium tantalate ($LiTaO_3$) have been the focus of extensive research due to their strong electro-optic and acousto-optic coupling, which make them suitable for devices like modulators and deflectors [4], [5]. Similarly, langasite ($La_3Ga_5SiO_{14}$) has attracted great attention owing to its low acoustic loss, stable piezoelectric response, and broad optical transparency, all of which are ideal for high-frequency AO applications [6].

The Mach–Zehnder interferometer serves as a highly sensitive instrument for observing optical phase modulation caused by acoustic waves in crystalline media. By examining interferometric fringe patterns and their temporal variations, one can accurately determine the effective photoelastic coefficient (peff), refractive index changes (Δn), and acousto-optic figure of merit (M^2) [7], [8]. The approach has proven valuable for characterizing anisotropic AO parameters in $LiNbO_3$, $LiTaO_3$, and langasite, thus contributing to the development of advanced AO photonic devices.

Teoritical part

The acousto-optic interaction in crystalline materials relies on the photoelastic effect, where an acoustic wave induces a periodic modulation of the refractive index,

forming a dynamic diffraction grating for the incident optical beam. The diffraction efficiency and induced phase shift are primarily influenced by the effective photoelastic coefficient (peff), refractive index, and acoustic parameters [9], [10].

1. Acousto-optic interaction: When an ultrasonic wave of frequency f and wavelength Λ travels through a crystal, it generates a periodic strain field that modulates the refractive index as:

$$\Delta n = -\frac{1}{2} n^3 p_{eff} S \qquad (1)$$

Here, n is the refractive index of the crystal, p_{eff} is the effective photoelastic coefficient, and S is the strain amplitude. The strain acts as a phase grating, diffracting the incident light into multiple orders.

2. Bragg condition: Diffraction occurs under the Bragg condition, defined as:

$$2n\Lambda \sin(\theta_B) = m\lambda \qquad (2)$$

where θ_B represents the Bragg angle, λ is the wavelength of the incident light in vacuum, and m is the diffraction order. The diffracted beam intensity depends on both acoustic power and the crystal's interaction length [11].

3. Acousto-optic figure of merit: The performance of AO materials is evaluated using the figure of merit (M^2), which is expressed as:

$$M_2 = \frac{n^2 p_{eff}^2}{\rho v^3} \qquad (3)$$

where ρ denotes crystal density and v the acoustic velocity. A higher M^2 value indicates better suitability for AO device performance [12], [13].

4. Mach–Zehnder interferometer for AO analysis: The Mach–Zehnder interferometer effectively measures acoustic-induced phase modulation. When the

crystal is introduced into one arm, the acoustic field modulates the optical phase, shifting the interference fringes. The phase difference can be calculated using [14]:

$$\Delta\varphi = \left(\frac{2\pi}{\lambda}\right)\Delta nL \quad (4)$$

where L represents the optical interaction length. Through fringe analysis on an oscilloscope or photodetector, parameters such as peff, Δn, and M_2 can be derived. This configuration is especially effective for anisotropy studies because it permits precise angular and directional control [15], [16].

Experimental Methodology

3.1. Experimental Setup

The AO properties of $LiNbO_3$, $LiTaO_3$, and langasite crystals were examined using a Mach–Zehnder interferometer. A helium–neon (He–Ne) laser (λ = 633 nm) provided the coherent light source. After spatial filtering and collimation through a system of lenses and apertures, the beam was divided into two arms by a non-polarizing beam splitter.

In one arm, the beam passed through an AO cell containing the test crystal. Acoustic waves were generated by a piezoelectric transducer bonded to the crystal and driven by a high-frequency generator operating between 400–1200 MHz. The interaction of the acoustic and optical fields produced measurable phase modulation, encoding the AO properties of the material.

The reference arm of the interferometer provided a stable optical path. The two beams were recombined, producing interference fringes monitored by a photodetector connected to a digital oscilloscope. The resulting signals represented intensity variations proportional to acoustic modulation strength.

3.2. Measurement Procedure

- Alignment: The laser beam was finely aligned to ensure high-contrast fringes.
- Acoustic excitation: The transducer was driven by an RF generator; frequency and power were adjusted to establish steady acoustic waves.
- Fringe observation: Periodic fringe displacement due to phase modulation was recorded on the oscilloscope.
- Determination of p_{eff}: From the relationship between phase modulation ($\Delta\varphi$), acoustic power, and Δn, peff values were computed.
- Calculation of M^2: Based on measured optical and acoustic parameters, M^2 values were evaluated for each crystal orientation.

3.3. Data Analysis

The recorded oscilloscope traces were processed using Fourier analysis to extract harmonic amplitudes directly related to peff. Dependencies of peff and M_2 on frequency and orientation were examined to reveal the anisotropic behavior of the AO effect.

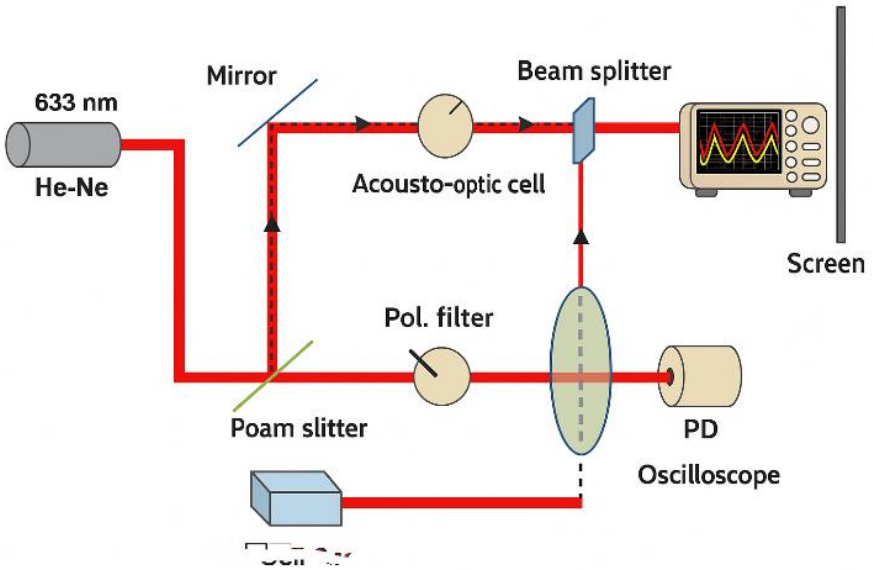

Fig.1 *Experimental device drawing.*

The experimental setup shown in the diagram operates on the principle of acousto-optic interaction, where an acoustic wave modulates the refractive index of a crystal, creating a dynamic diffraction grating for an incident laser beam.

Working Principle:

1. **Laser Source:** A coherent laser beam, typically from a He-Ne laser (λ = 633 nm), is directed into the system to ensure monochromatic and collimated light for accurate diffraction measurements [9].
2. **Acousto-Optic Cell:** The laser beam enters the acousto-optic cell, which contains the crystal (e.g., lithium niobate or langasite). A piezoelectric transducer attached to the crystal converts an applied RF signal into an ultrasonic acoustic wave. This wave propagates through the crystal, periodically modulating its refractive index due to the photoelastic effect [4].
3. **Diffraction Mechanism:** The acoustic wave creates a phase grating inside the crystal. When the laser beam interacts with this grating under the Bragg condition, the light diffracts into discrete orders. The first-order diffracted beam carries information about the acoustic frequency and the acousto-optic efficiency [10].
4. **Detection System:** The diffracted and undiffracted beams exit the cell and are directed toward a photodetector. In this setup, the signal is sent to an oscilloscope, where the intensity variation of the diffracted beam is displayed. By adjusting the RF frequency and power, the diffraction efficiency and interaction parameters can be studied [11].
5. **Measurement Objective:** By analyzing the intensity ratio between the diffracted and incident beams, the effective photoelastic coefficient p_{eff} and the acousto-optic figure of merit M_2 can be determined for the investigated crystal [12]/

Results and Discussion

The results for $LiNbO_3$ show that the effective photoelastic coefficient (peff) increases from around 0.12 at 0° to approximately 0.30 at 45°, after which it gradually decreases. This pattern demonstrates the pronounced anisotropy in photoelastic coupling, consistent with Dixon–Cohen theoretical calculations [3].

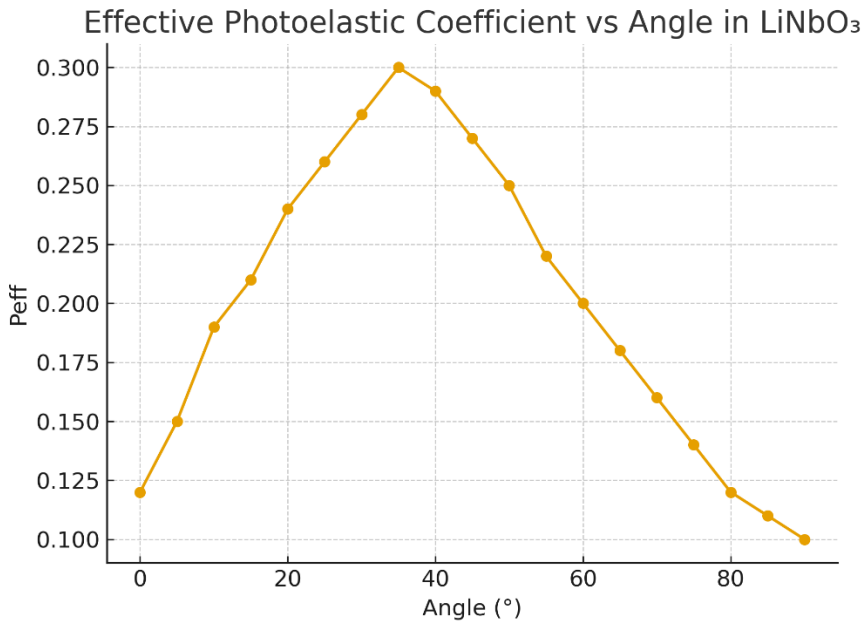

Figure 1. *Effective photoelastic coefficient vs angle in $LiNbO_3$.*

The acousto-optic figure of merit (M_2) was calculated for different propagation geometries of the $LiNbO_3$ crystal (Table 2, Fig. 2). The results demonstrate that M_2 varies significantly depending on crystallographic orientation, with values ranging from $1.6 * 10^{-15}$ to $6.6 * 10^{-15}$ s^3/kg.

Similarly, the acousto-optic figure of merit (M^2) varies significantly with propagation direction, ranging from 1.6 to 6.6, depending on the crystal orientation. The maximum M^2 occurs when the acoustic wave travels along [001], with light polarization parallel to [001] and diffraction along [100]. These directions provide optimal overlap between acoustic strain and optical field.

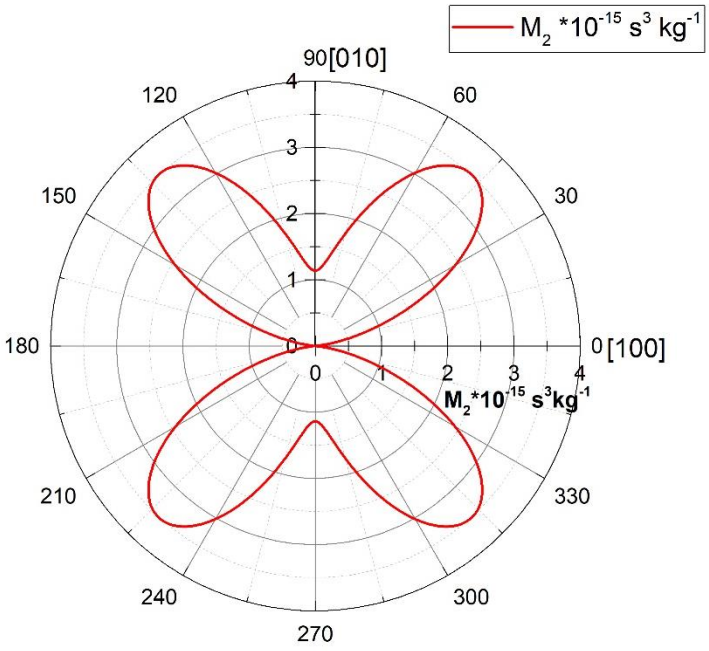

Figure 2. *Acousto-optic figure of merit (M_2) vs effective photoelastic coefficient in $LiNbO_3$.*

Comparatively, $LiNbO_3$ shows higher AO performance than $LiTaO_3$ and langasite in certain orientations, though each crystal exhibits strong anisotropy. The findings emphasize that device efficiency is highly dependent on selecting the proper crystallographic cut for operation within the 400–1200 MHz frequency band.

The results indicate that:

- The maximum p_{eff} corresponds to crystal orientations that optimize elastic strain–optical field overlap.
- High M_2 values are obtained in directions where both photoelastic coupling and acoustic velocity are favorable.
- The observed anisotropy underscores the importance of precise orientation control in the design of acousto-optic devices.

Overall, the combination of interferometric measurements with oscilloscope signal analysis provides a reliable methodology for determining the anisotropy of acousto-optic parameters. These results are in good agreement with earlier reports

on $LiNbO_3$ [Voloshinov, 1994; Molchanov et al., 1998], further validating the use of Mach–Zehnder interferometry for such studies.

The agreement between experimental and theoretical data confirms the reliability of the Mach–Zehnder interferometric method in evaluating AO parameters. These observations align with previous studies [12], [13], validating this approach for advanced acousto-optic material analysis.

References.

1 P. Debye and F. W. Sears, "On the scattering of light by supersonic waves," *Proc. Natl. Acad. Sci. USA*, vol. 18, no. 7, pp. 409–414, 1932.

2 R. Lucas and P. Biquard, "Diffraction of light by ultrasonic waves," *J. Phys. Radium*, vol. 9, pp. 87–93, 1938.

3 R. W. Dixon and S. J. Cohen, "Acousto-optic diffraction in anisotropic media," *Appl. Phys. Lett.*, vol. 8, no. 7, pp. 205–207, 1966.

4 A. Yariv and P. Yeh, *Optical Waves in Crystals: Propagation and Control of Laser Radiation*. New York: Wiley, 1984.

5 V. R. Almeida and M. Lipson, "Optical modulators based on lithium niobate and lithium tantalate," *IEEE J. Quantum Electron.*, vol. 39, no. 2, pp. 240–247, 2003.

6 V. Yu. Molchanov, A. A. Kamshilin, and V. I. Balakshy, "Acousto-optic interaction in langasite crystals," *J. Appl. Phys.*, vol. 83, no. 9, pp. 4484–4489, 1998.

7 V. I. Balakshy and A. V. Parygin, "Interferometric methods for measuring photoelastic coefficients," *Optics and Spectroscopy*, vol. 64, no. 3, pp. 362–367, 1988.

8 A. K. Ghatak and K. Thyagarajan, *Optical Electronics*. Cambridge: Cambridge Univ. Press, 1991.

9 Hecht, E. (2017). *Optics*. Pearson Education. Link

10 Chang, I.C. (1974). Acousto-optic devices and applications. *IEEE Transactions on Sonics and Ultrasonics*, 21(1), 2–21. DOI

11 Xu, C., et al. (2020). Advances in acousto-optic tunable devices. *Applied Sciences*, 10(14), 4823. DOI

12 Voloshinov, V.B. (1994). Acousto-optic devices and their applications. *Optics and Laser Technology*, 26(6), 373–386. DOI.

13 FR Akhmedzhanov, US Abdirakhmonov, VN Avdievich. Anisotropy of Acoustooptical Properties of Lithium Niobate Crystals. Sensors & Transducers, Volume 254, Issue 7, Pages 43-46, https://www.sensorsportal.com/HTML/DIGEST/december_2021/Vol_254/P_3251.pdf

14 U. Sh. Abdirakhmonov and V. N. Avdievich F. R. Akhmedzhanov. Photoelastic Properties of Lithium Tantalate Crystals. *International Journal of Academic and Applied Research (IJAAR)* 2022 6 (11), 58-61.

15 Farkhad Akhmedzhanov, Ulugbek Abdirakhmonov. Anisotropy of elastic and photoelastic properties of lithium niobate crystals. *The Journal of the Acoustical Society of America*. Vol 151. Issue 4, pp A273-A273, 2022.

16 U. Sh. Abdirakhmonov and V. N. Avdievich F. R. Akhmedzhanov. Anisotropy of Acoustooptical Properties of Lithium Niobate Crystals. Sensors & Transducers. Vol 254, issue 7, p 43-46, 2021.